Available online at www.eccomasproceedia.org
Eccomas Proceedia COMPDYN (2017) 4778-4795

ECCOMAS
Proceedia

COMPDYN 2017
6th ECCOMAS Thematic Conference on
Computational Methods in Structural Dynamics and Earthquake Engineering
M. Papadrakakis, M. Fragiadakis (eds.)
Rhodes Island, Greece, 15–17 June 2017

VIBRATION ATTENUATION IN PIPES: DESIGN AND EXPERIMENTAL VALIDATION OF A RESONANT METAMATERIAL SOLUTION

A. Nateghi[1*], L. Sangiuliano[1, 2], C. Claeys[1, 2], E. Deckers[1, 2], B. Pluymers[1, 2], W. Desmet[1, 2]

[1] KU Leuven, Department Mechanical Engineering
Celestijnenlaan 300, box 2420, 3001 Heverlee, Belgium
{alireza.nateghi, luca.sangiuliano, claus.claeys, elke.deckers, bert.pluymers,
wim.desmet}@kuleuven.be

[2] Member of Flanders Make

Keywords: Resonant Metamaterial, Bloch-Floquet Theorem, Mechanical Vibration, Wave Propagation, Stopband Zone.

Abstract. *In recent years, locally resonant metamaterials have shown great potential in efficiently attenuating mechanical vibrations and providing noise insulation in various applications. Given the wide application range of lightweight pipes and considering that such structures can serve as excellent waveguides as they are often quite long, a locally resonant metamaterial pipe is presented in this paper. This metamaterial solution is chosen to investigate whether it is possible to use the metamaterial concept on pipe-like structures. Resonators are added to the pipe on a subwavelength scale in order to create a stopband zone in the propagation of flexural waves. Utilizing the Bloch-Floquet theorem and considering a periodic distribution of the local resonators, unit cell modelling is adopted to design the metamaterial pipe with a stopband zone in the frequency range of interest. Only a limited number of resonators are added to the original pipe in order to keep the added mass ratio due to these resonators below 10%. The results obtained from Bloch-Floquet theorem hold for an infinite metamaterial pipe with a periodic distribution of local resonators, but previous studies have shown that they provide a reliable prediction of the zone of highly attenuated response of the finite structure as well. Finally, the metamaterial pipe is manufactured to experimentally validate the results provided by the numerical prediction of the stopband zone. The metamaterial structure is composed of an Aluminum pipe as the host structure with added local resonators which are produced from Plexiglas using a laser cutting technique. The experimental results prove the existence of the stopband zone as predicted by the unit cell analysis of the infinite metamaterial pipe. The proposed concept provides an easy-to-apply metamaterial solution which can provide the stopband behavior while meeting the lightweight criterion.*

Peer-review under responsibility of the organizing committee of COMPDYN 2017.
doi: 10.7712/120117.5761.17379

1 INTRODUCTION

In recent years, there has been an increasing interest in innovative lightweight designs in various applications. However, these lightweight solutions often show unfavorable Noise, Vibration and Harshness (NVH) behavior and given the impact of noise pollution on human health [1], a search for innovative solutions which both meet the lightweight criterion and satisfy NVH requirements has started. These novel NVH solutions need to be kept simple, cheap and fairly easy to apply. One of such novel solutions is the locally resonant metamaterials.

In recent years, locally resonant metamaterials have been in the spotlight as possible solutions for vibration attenuation and sound insulation problems, be it in targeted frequency ranges [2, 3]. Locally resonant metamaterials generally function by creating a stopband zone in which the structure does not support free wave propagation. This behavior in metamaterials is obtained due to the addition of local resonators to the host structure resulting in the destructive interference between the on-going waves propagating in the structure and the waves reradiated from the resonant cells within the stopband zone [4]. This new family has shown potential in efficiently controlling acoustic radiation and sound transmission while satisfying the lightweight requirement [5]. The potential of locally resonant metamaterials in vibration attenuation has recently been studied by Claeys et al. [6]. It is worth noting that the stopband behavior in locally resonant metamaterials is not dependent on the periodicity of the structure.

In recent years, academic verification of locally resonant metamaterials has been performed [6 - 8]. In such studies, the resonant cells are modelled as grids of mass-spring systems added to the hosting structure. However, there have also been a number of investigations on the feasibility of locally resonant metamaterials as realizable NVH problems. In one of such studies, Claeys et al. have proposed a design for resonant cells which can be realized fairly easily while meeting the lightweight criterion and providing favorable NVH behavior [9, 10]. Their study proves the increased acoustic insertion loss of a finite enclosure due to the addition of the resonant cells.

As stated, periodicity is not a required property of locally resonant metamaterials; however, assuming a periodic distribution of the resonant cells, has its benefits in modelling efficiently. Assuming an infinite periodic structure, wave motion in the structure can be characterized by investigation of a unit cell and applying the Bloch-Floquet theorem [11, 12]. A unit cell is defined as a smallest portion of a periodic structure which contains all the essential information required to describe wave propagation through the entire structure. In the context of metamaterials, wave propagation in the structure is commonly described using dispersion curves which relate wavenumbers of propagating waves to the frequency at which they propagate. Application of the Bloch-Floquet theorem and unit cell modelling in the design of periodic structures has been thoroughly investigated [13, 14].

Studies on wave propagation in curved structures show that the behavior of such structures significantly differ from their planar counterparts as e.g. shown in [15]. Therefore, next to studies on the stopband behavior in flat metamaterial plates, it is worth to investigate the effect of curvature on the behavior of locally resonant metamaterials. Recently, Nateghi et al. [16, 17] extended the metamaterial demonstration of Claeys et al. [9] to the case of infinite cylindrical shells and pipes. The results show a considerable difference in behavior due to the addition of the cylindrical curvature and the existence of cut-on frequencies. It was shown that below cut-on frequencies of flexural waves the behavior of cylindrical and flat metamaterial structures differ considerably. In addition, it is observed that addition of local resonators to the cylindrical host influences the cut-on frequency of the flexural waves; especially in the vicinity of the targeted stopband zone. Moreover, it was observed that the frequency range of the stopband of flexural modes with different circumferential wavenumbers differ from each

other. However, the overall dynamic behavior of the cylindrical structure is improved as the stopband zone is obtained.

In this paper, wave motion in locally resonant metamaterial pipes is investigated. Following form the findings of [17], a metamaterial solution for vibration attenuation of a lightweight Aluminum pipe is designed, analyzed and produced. To this end, first, a new resonant structure is designed and then, utilizing the Bloch-Floquet theorem and assuming a periodic distribution of the resonant cells through the pipe, the effects of these resonators on the structure are investigated. In this step, the dispersion curves of the metamaterial pipe are obtained and stopband zones are numerically predicted. In the next step, the metamaterial pipe is produced and an experimental set-up is designed to validate the numerical prediction. In this study, the metamaterial structure is composed of a hosting Aluminum pipe of 1 m length which is treated by gluing on Poly(Methyl Methacrylate), also known as PMMA, resonant cells, produced using a laser cutting technique. The experimental results prove the existence of a stopband zone due to the addition of the resonant cells to the pipe and the frequency range of the stopband zone is in good agreement with the unit cell modelling prediction.

The paper is structured as follows. Section 2 discusses the application case in more details. Section 3 describes the metamaterial solution and the overall design of the resonant cells. Section 4 briefly explains the application of unit cell modelling on the resonant cells described in section 3. Dispersion curves are obtained and the stopband is predicted. Section 5 provides information on the specifications of the experimental set-up and the experimental results are discussed in section 6. Finally, the main conclusions of the research are drawn and discussed.

2 HOST STRUCTURE

A lightweight thin pipe is chosen as a case study because of its wide range of applications; from piping networks to rotating machinery amongst other applications. Considering the low mass of the structure, its hollowness and the fact that it is quite thin, the radiated noise from the wall of such a pipe can be considerable [18] . Moreover, as shown in [17], the circular curvature of the structure is a good demonstration of the effect of curvature on the metamaterial solution and stopband zones.

In the current study, an Aluminum pipe of length 1 m, thickness 2.1 mm and inner radius of 4.8 cm is chosen as the case study. The choice of Aluminum is due to its common usage in industrial applications from transportation industry to various piping systems. The mechanical and physical properties of the Aluminum pipe is given in Table 1. Considering the importance of NVH behavior at lower frequencies, the behavior of the structure below 1000 Hz is targeted and investigated.

Material	Young's modulus [GPa]	Poisson's ratio [-]	Density [kg/m^3]
Aluminum	68	0.35	2696.2
PMMA	4.85	0.31	1188.38

Table 1: Material properties of the Aluminum pipe and the PMMA resonant cells.

3 LOCALLY RESONANT METAMATERIAL PIPE

In this section, the design of the metamaterial solution is explained in more detail. The main interest of this paper is to improve NVH behavior of a thin Aluminum pipe as a lightweight hollow structure. To this end, considering the importance of the flexural waves on acoustic radiation of structures, in this work, creating a stopband zone in the propagation of

the flexural waves is targeted. To this end, resonant cells are designed to have a low-frequent flexural mode and are added to the host structure on a subwavelength scale to satisfy the criteria of metamaterial design [2].

In the current work, the metamaterial structure is composed of the Aluminum pipe introduced in section 2 as the host structure with the addition of resonant cells produced from a PMMA panel using laser cutting technique. The representation of such a resonant cell is shown in Fig. (1). The mechanical and physical properties of the resonant cells are given in Table 1. These parameters are retrieved through correlation of the measured frequency response of the structure with the frequency response predicted by the numerical model.

The dimensions of the resonant cells should be chosen based on the frequency range of the intended stopband zone as this zone occurs around the first flexural eigenfrequency of the resonator. The goal in this research is to keep the added mass ratio of the resonant cells to the host structure low to make sure that the metamaterial solution still falls under the definition of a lightweight solution.

The resonators are tuned to have their first flexural resonant frequency around 800 Hz and therefore the geometrical parameters shown in the second row of Table 2 are chosen for the resonant cell shown in Fig. (1). This frequency range is chosen as numerical simulations of the Aluminum pipe show a vibrating mode which can contribute to acoustic radiation at 800 Hz. However, after production of the cells, measuring the final geometrical parameters of 5 samples and averaging these data provides the updated geometrical parameters of the resonant cells which are used in the numerical prediction of the stopband zones. These updated parameters are given in the last row of Table 2.

A similar design as in [10, 19] is used in this research as shown in Fig. (1). Note that the thickness of the resonator is kept constant and equal to 8 mm. The chosen shape makes the production of the resonant cells through laser cutting straightforward.

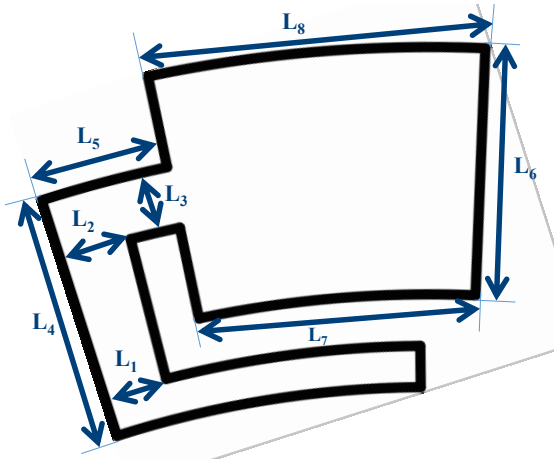

Figure 1: Representation of the resonant cells.

Dimensions [mm]	L_1	L_2	L_3	L_4	L_5	L_6	L_7	L_8
Designed	3.12	3.54	3.00	12.00	7.36	12.00	13.51	16.49
Measured	2.97	3.21	2.76	11.83	7.47	11.75	13.56	15.95

Table 2: Geometrical parameters of the resonant cell shown in Fig. (1).

The resonant cell is modelled using the properties and the dimensions stated in Tables 1 and 2 in COMSOL Multiphysics. The model is discretized using 12440 quadratic tetrahedral solid elements resulting in 62253 degrees of freedom. Note that fixed boundary conditions are assumed at the base of the resonator. As it can be seen from Fig. (2), the first eigenfrequency of the resonator is a flexural mode with respect to the host structure and it occurs at 745.8 Hz, while the second eigenfrequency occurs at 1059.1 Hz and can be described as a longitudinal mode with respect to the host structure. Following previous studies [9, 17], it will be investigated both numerically and experimentally whether the addition of this type of resonator to a pipe can induce a stopband.

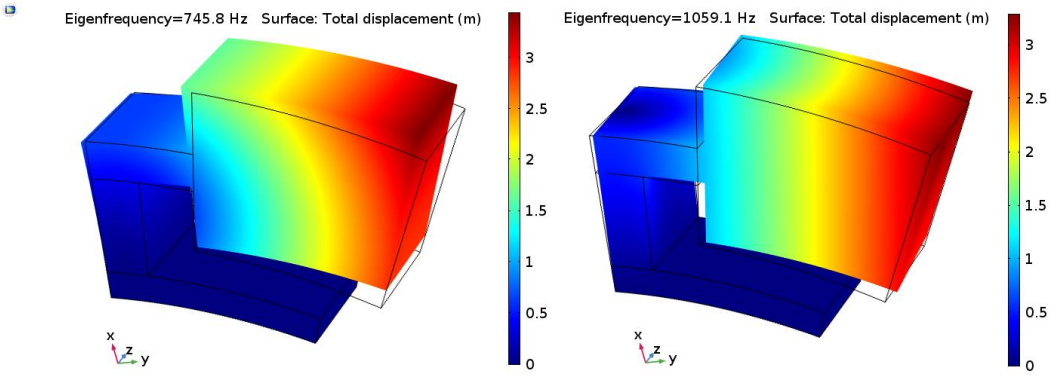

Figure 2: Modeshapes of the first and second eignfrequencies of the resonant cells. The wireframe represents the undeformed state of the resonant cells.

4 UNIT CELL MODELLING AND STOPBAND ZONE

Next step in the investigation of the stopband behavior of the locally resonant metamaterial pipe is a wave dispersion analysis. As stated before, at this step, it is assumed that the resonant cells are distributed periodically over the pipe on a subwavelength scale. The grid for such a periodic distribution is also of importance. It is assumed that 8 resonant cells are distributed around the circumference of the pipe and this ring of resonance cells is infinitely repeated in the axial direction. The distance between two resonators in the axial direction is 4 cm. Fig. (3) shows the representative unit cell which is used in the dispersion analysis. Also the host structure is accounted for in the unit cell.

After choosing the proper representative unit cell, it is possible to apply the Bloch-Floquet theorem to obtain dispersion curves which provide the required information on wave propagation through the infinite structure. These dispersion curves provide the relationship between the wavenumbers and the frequency of the waves which can propagate in the structure. The application of Bloch-Floquet theorem for the dispersion analysis of both open cylindrical metamaterial shells and metamaterial pipes are performed by Nateghi et al. [16, 17]. Considering the configuration used in the current study, readers are referred to [17] for the required formulations of unit cell modelling in infinitely long cylindrical pipes. Based on this formulation, for the dispersion analysis of the metamaterial pipe, it is required to set integer values to the circumferential wavenumber k_φ as shown in Fig. (4) and solve the remaining quadratic eigenvalue problem for the values of the axial wavenumber k_z which then provide dispersion curves. The stopband zones appear as discontinuities in the dispersion curves of the corresponding waves. This zone indicates a frequency range in which no solution exists as the free wave propagation in the structure is hindered.

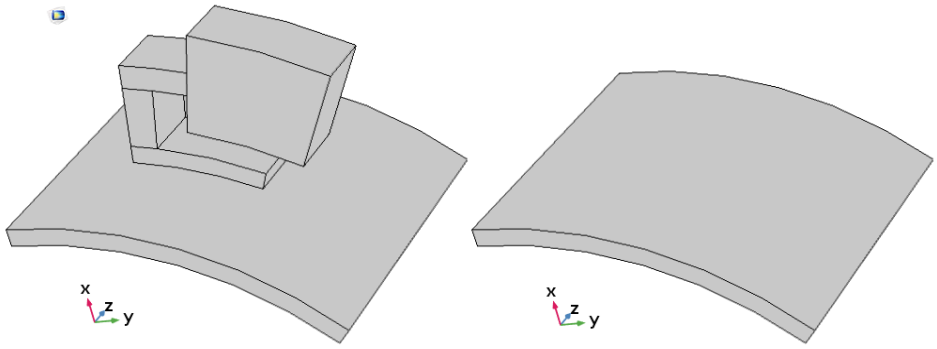

Figure 3: Representative unit cell of the metamaterial pipe (left) and the host Aluminum pipe (right).

It is more convenient to analyze the wave propagation vector $\boldsymbol{\mu} = \boldsymbol{k}.\boldsymbol{d}$ instead of the wavenumber vector $\boldsymbol{k}$ given since it is a non-dimensional vector with $\boldsymbol{d}$ the lattice basis vector. In addition, in this analysis, only real wave vectors, corresponding to free propagating waves, are considered. In the current section, only the real parts of the solutions are represented as they provide sufficient information for stopband prediction.

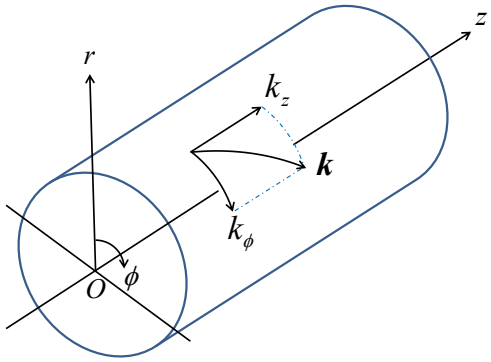

Figure 4: Representation of the wavenumber vector in a pipe as shown in [17].

The unit cell models of Fig. (3) are modelled in COMSOL Multiphysics and periodic boundary conditions are applied to the unit cell model. Afterwards, following the formulations provided in [17] the dispersion relation is solved for the axial wavenumbers of propagating waves at fixed frequencies and circumferential wavenumbers. Given the imposed periodic boundary condition, solving the dispersion relation provides a periodic set of solutions in the wavenumber domain. This periodic set of solutions in the wavenumber domain has the intervals of $\left[-\frac{\pi}{L},\frac{\pi}{L}\right]$ in which L is the length of the unit cell in the axial direction.

In the next subsections, first the dispersion curves representing wave propagation through the hosting pipe are discussed to further understand wave motion in the Aluminum pipe. Afterwards, the unit cell model consisting of the Aluminum pipe and the resonant cell is studied to provide a numerical prediction of the frequency range of the stopband zone.

4.1 Wave propagation in the host structure

Fig. (5) shows dispersion curves of the propagating parts of the waves with the circumferential wavenumber k_φ=0, 1 and 2 rad/rad in an infinite Aluminum pipe represented by the host unit cell of Fig. (3). These curves represent breathing, beam bending and ovalling modes of vibration in the pipe, respectively. In this figure, only the propagating parts of the waves are

depicted as their information suffices for the purpose of stopband detection. It is worth mentioning that in the dispersion curves of the metamaterial pipe, the stopband appears as a discontinuity in the dispersion curves of the flexural waves.

As it can be seen in the dispersion curves representing the breathing mode, two pairs of waves can propagate through the structure within the frequency range of 0 Hz – 1000 Hz which correspond to the longitudinal and shear modes of vibration. The dispersion curves representing flexural waves do not appear in this frequency range as the flexural wave of the breathing mode is only cut on at 17417 Hz. It is worth mentioning that although, breathing mode has a considerable contribution to acoustic radiation, given that the stopband of the current work is targeting propagating flexural waves around 750 Hz, this mode is not of high importance in stopband prediction as the flexural wave has not cut on in this frequency range.

Based on the dispersion curves of the ovalling and beam bending modes, only flexural waves are propagating in this frequency range. Considering the current resonator design, these are the waves that are targeted in the current study. It is worth mentioning that waves with higher circumferential wavenumbers are not investigated as their flexural waves cut on at frequencies higher than 1000 Hz.

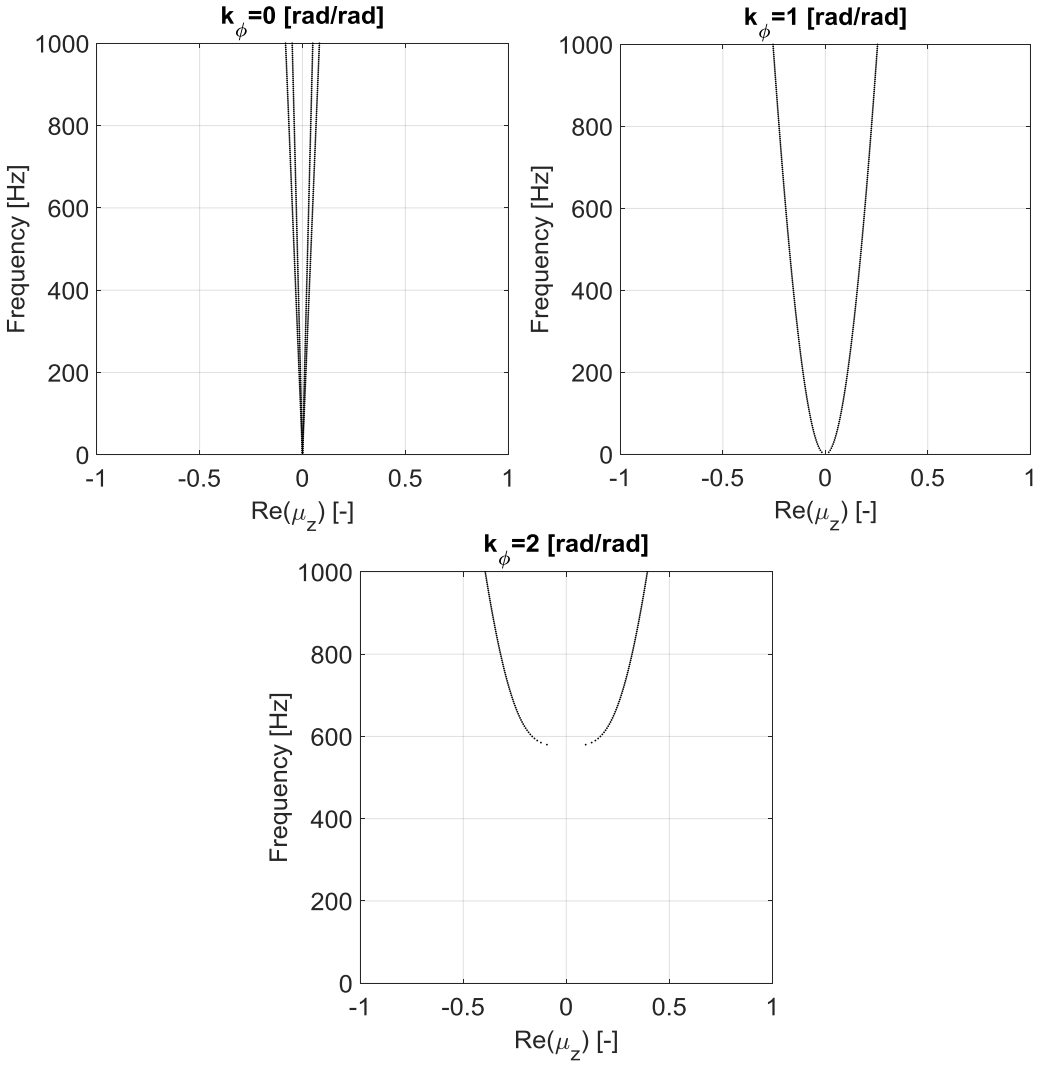

Figure 5: Dispersion curves representing wave motion in the infinite bare Aluminum pipe with circumferential wavenumbers 0, 1 and 2.

4.2 Wave propagation in the metamaterial pipe

Dispersion curves of the propagating waves with k_φ=0, 1 and 2 rad/rad obtained from the representative unit cell of the metamaterial pipe (as shown in Fig. (3)) are given by Fig. (6). As it can be seen from the figure, the addition of the resonant cells have influenced the dispersion curves representing the wave propagation of the breathing mode even though the flexural waves have not cut on below 1000 Hz. This effect can be explained based on mode coupling and the wave propagation related to the motion of the local resonant cells at the eigenfrequency of the resonators [17]. It has been shown that below the ring frequency, i.e. the cut-on frequency of the flexural wave of the breathing mode, waves are not of pure flexural, shear and longitudinal nature.

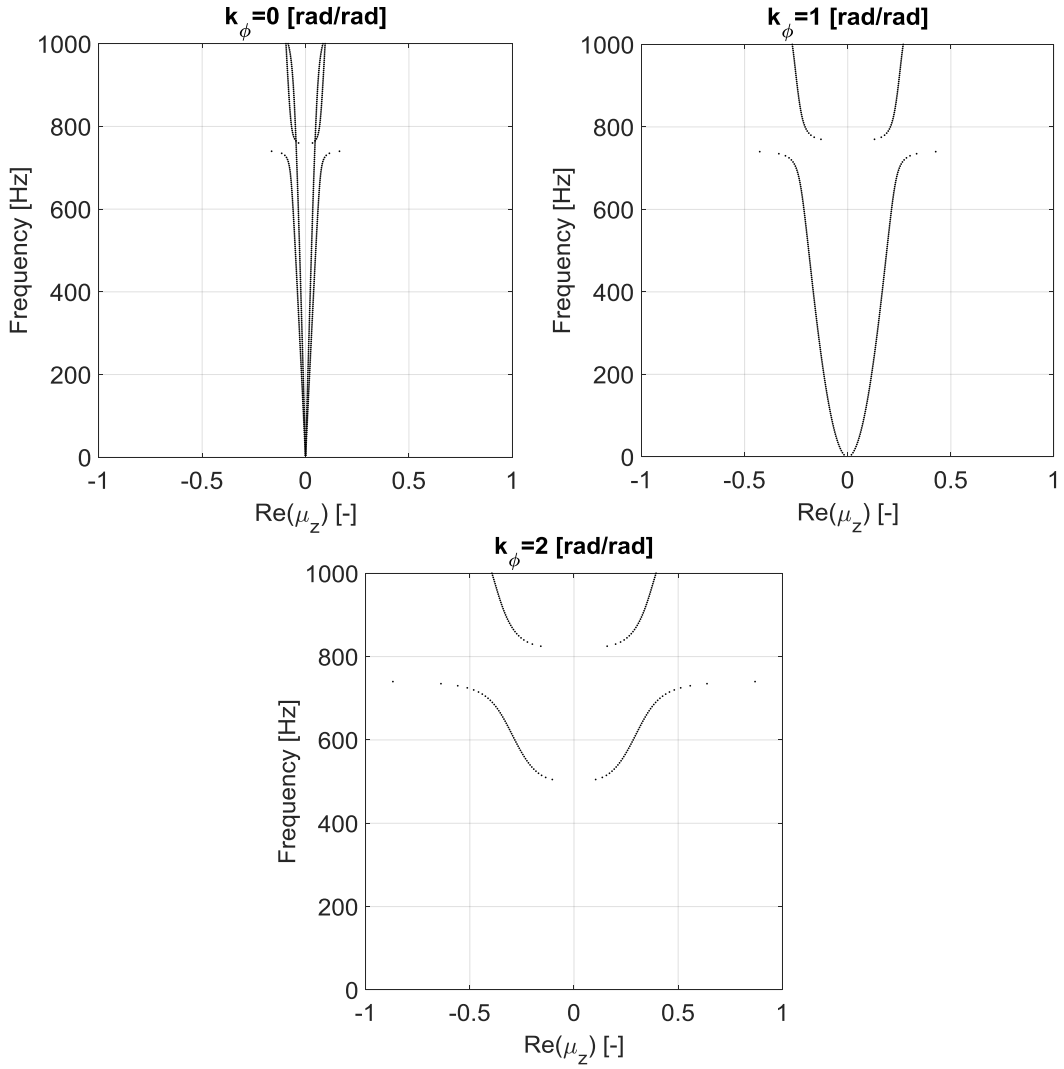

Figure 6: Dispersion curves representing wave motion in the infinite metamaterial pipe with circumferential wavenumbers 0, 1 and 2.

The dispersion curves of the beam bending and ovalling modes show a clear gap in the curves representing the propagating flexural waves. These gaps prove the existence of stopband zones due to the addition of the local resonators and are in the frequency ranges of 740 Hz - 770 Hz and 740 Hz - 825 Hz for beam bending and ovalling modes, respectively. Therefore, based on these results it can predicted that the current design creates an overall stopband

zone between 740 Hz and 770 Hz. It is expected that a significant attenuation can be obtained between 740 Hz - 825 Hz by applying this metamaterial solution to the Aluminum pipe.

Another point of interest in the dispersion curves shown in Fig. (6) is related to the cut on frequency of the flexural wave in the ovalling mode which is affected due to the addition of the resonant cells. In previous studies, it has been shown that below the stopband zone, the addition of the local resonators pushes the cut on frequency of the propagating waves to lower frequencies while above the stopband zone the cut on frequencies of waves increase. Readers are referred to [16] for further information in this regard.

5 EXPERIMENTAL SET-UP

This section provides information on the production aspect of the metamaterial pipe and explains the specifications of the test set-up.

5.1 Production of the resonators

The resonant cells are produced from PMMA panels as shown in Fig. (7), using a laser cutter machine. The resonators are all cut from the same panel using the same laser cutter tool to try to keep the material properties and the possible production errors as consistent as possible. However, there is still a deviation between the geometries of the designed and finally produced parts.

Figure 7: Produced PMMA resonators.

As already explained in section 3, the final geometrical parameters of the produced resonators are measured and averaged using 5 separate samples and are given in Table 2. In order to be sure about the actual resonance frequency of the produced parts, an experiment is performed using a Scanning Laser Doppler Vibrometer (SLDV) as shown in Fig. (8). 5 samples of the produced resonators are chosen and glued to a rigid plate. In order to make the contact between the rigid part and the resonant cells more consistent, the resonator design is changed slightly by making their base flat as shown in the figure. Numerical simulations show that the influence of this design change on the resonance frequency of the parts is negligible; considering that the change is limited to the base of the cells which is glued to the rigid part. The rigid structure is mounted on and excited by a shaker The acceleration of the tip of the resonators due to the shaker excitation is measured using SLDV as shown in the figure.

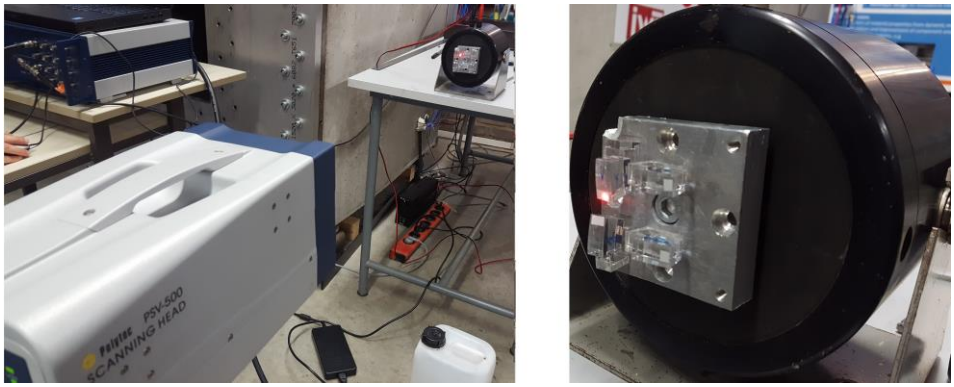

Figure 8: SLDV set-up for flexural eigenfrequency measurement of 5 of the resonators.

Fig. (9) shows the measured acceleration of five resonators in the frequency range of 0 Hz -1000 Hz. As it can be observed, there is a clear resonance frequency between 735 Hz – 743 Hz which shows up as a peak in the figure. From these five samples, it can be concluded that the average resonance frequency of the produced parts lies at 740 Hz which is in good agreement with the results of the numerical simulations. It is worth noting that the scatter in the resonance frequency of the produced parts can affect the performance of the metamaterial solution in the stopband zone and it is important to reduce it as much as possible. However, in the current case, the scatter of 8 Hz with a maximum relative error of 0.68% with respect to the average resonance frequency seems to be in an acceptable range [20].

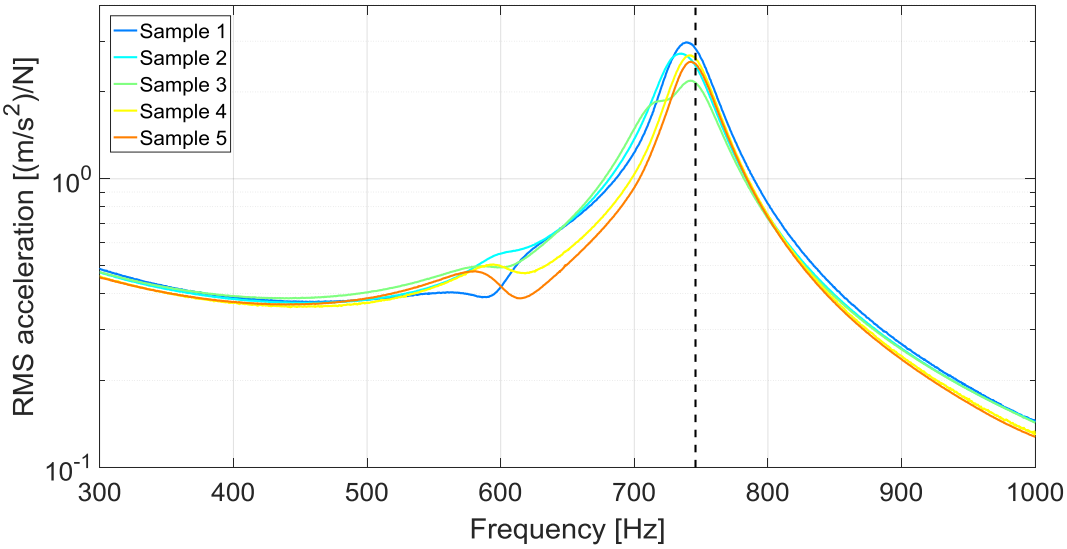

Figure 9: Frequency response of the produced PMMA resonators under shaker excitation measured by SLDV. Dashed line indicates the numerically predicted resonance frequency.

5.2 Test set-up

The test set-up used for the experimental frequency response analysis of the metamaterial pipe is described in this section. The test bench shown in Fig. (10) is used to mount the metamaterial pipe. It consists of a table with rigid stands from which the test specimen is suspended using guitar strings to limit the effects of possible coupled vibrations of the pipe and the table and to limit the effect of mounting conditions.

As excitation, a hammer is used to perform impact testing. To measure the response of the pipe, four lightweight accelerometers are attached to different sections of the pipe.. Each of the accelerometers weighs 0.8 g which makes the additional mass of them negligible as compared to the mass of the metamaterial pipe.

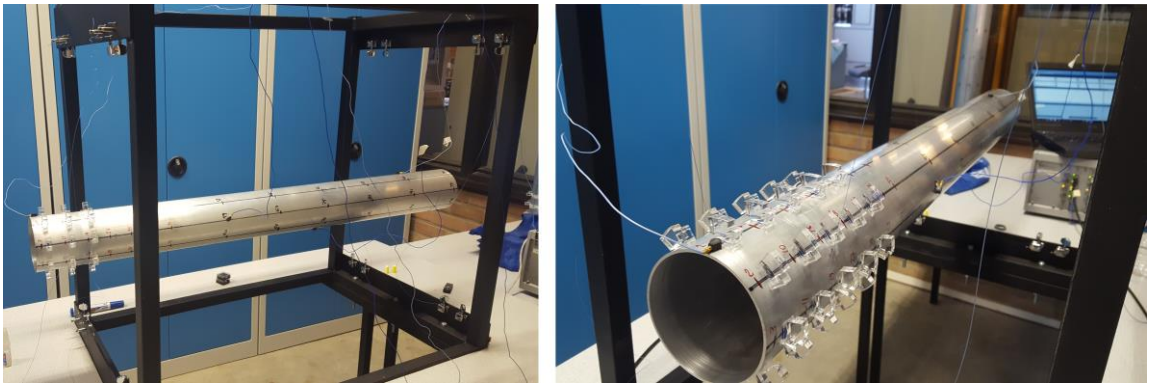

Figure 10: Test set-up.

In order to characterize wave propagation through the structure there is a need for various measurement points on the pipe. The roving hammer method is applied in order to avoid the need of adding many accelerometers. This means that the excitation location is varied and the response location is kept fixed as a reference. Due to the reciprocity principle, valid for linear systems, the response and input points can be interchanged.

The metamaterial pipe is divided into 13 sections as shown in Fig. (11) and on each section 8 equidistant points around the circumference are chosen, corresponding to a total of 104 excitation locations for the roving hammer. The acceleration response is measured at the 4 points shown in Fig. (11).

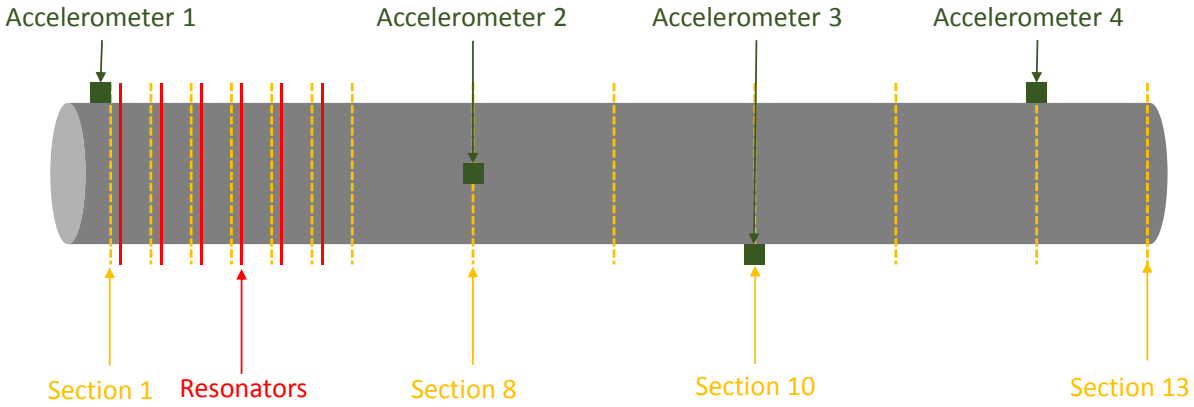

Figure 11: Excitation sections, measurement points and the location of resonators.

As indicated in figure (11) only six rings of resonators are glued to the Aluminum pipe and the rings are distributed evenly with 4 cm of distance between two rings. The number of resonator rings is chosen based on the results reported by [10] where 6 rows of resonators are shown to be sufficient to create stopband behavior. In order to fully capture the effect of the resonant cells on the behavior of the pipe, there are spatially more excitation sections foreseen in the left side of the pipe in order to characterize the decay of the waves passing through each ring of resonant cells. Furthermore, to evaluate the effect of each ring or resonators separately, the measurement procedure is repeated for 7 different configurations. First the bare case is

measured. Next the ring on the left side is added and the pipe is measured again. This procedure is repeated for the next 5 rings, where the rings are added consecutively from left to right.

The averaged measured mass of a single resonant cell is 2.24 g, summing up to a total added mass of 107.52 g for all 48 cells which are glued to the pipe in the final metamaterial design. With a total mass addition of 6.16% to the host structure, this can still be considered as a lightweight NVH treatment.

6 MEASUREMENT RESULTS AND DISCUSSION

Test results are discussed in this section. Applying the reciprocity principle, the results are given in the form of averaged measured RMS accelerations for the different sections of the pipe and averaged measured RMS accelerations of the entire pipe with respect to the location of the corresponding reference positions. RMS acceleration of different sections are calculated according to the following formula:

$$\left|H\right|_{\ddot{X}_{n/F_e,rms}} = \sqrt{\frac{1}{M}\sum_{k=1}^{M}\left|H\right|^2_{\ddot{X}_{n,k/F_e}}}, \tag{1}$$

in which $\left|H\right|_{\ddot{X}_{n,k/F_e}}$ indicates the amplitude of the acceleration frequency response in point k on section n for an excitation in point e and M is the number of points per section. Note that the RMS acceleration of the entire pipe is calculated as follows:

$$\left|H\right|_{\ddot{X}_{F_e,rms}} = \sqrt{\frac{1}{(N.M)}\sum_{n=1}^{N}\sum_{k=1}^{M}\left|H\right|^2_{\ddot{X}_{n,k/F_e}}}, \tag{2}$$

where N is the number of sections of the pipe. Fig. (12) shows the measured RMS acceleration of the entire pipe for the 7 configurations, based on input on the location of accelerometer 1. It is observed that between 700 Hz - 780 Hz, there is an obvious dip building up in the frequency response of the pipe which shows the existence of the stopband zone due to the addition of the resonators. The numerically predicted stopband is indicated by dashed lines and corresponds well to the measurements.

It is observed that the dip in the frequency response of the pipe within the stopband zone gets more pronounced with the addition of each resonator ring which indicates that the attenuation of the waves becomes stronger.

It is also noted that below the stopband zone there is a shift to the left in the frequency response of the pipe with the addition of the resonator cells which can be clearly observed in the peaks of the figure which represent different eigenmodes of vibration of the pipe. This shift for the eigenmode above stopband is towards higher frequencies. This behavior can be explained due to in-phase and out-of-phase motion of the pipe and the resonators below and above the stopband zone, respectively. It has been shown that below stopband zone, motion of the resonators and the host structure are in-phase resulting in a higher dynamic mass [9]. This higher dynamic mass shifts the eigenmodes of the host to lower frequencies while above stopband zone out-of-phase motion of the resonators and the host leads to the opposite effect.

In addition of the stopband zone, some clear reduction in the amplitude of these lower frequency modes is also observed which can be related to the added damping coming from the PMMA resonator cells and their moving masses.

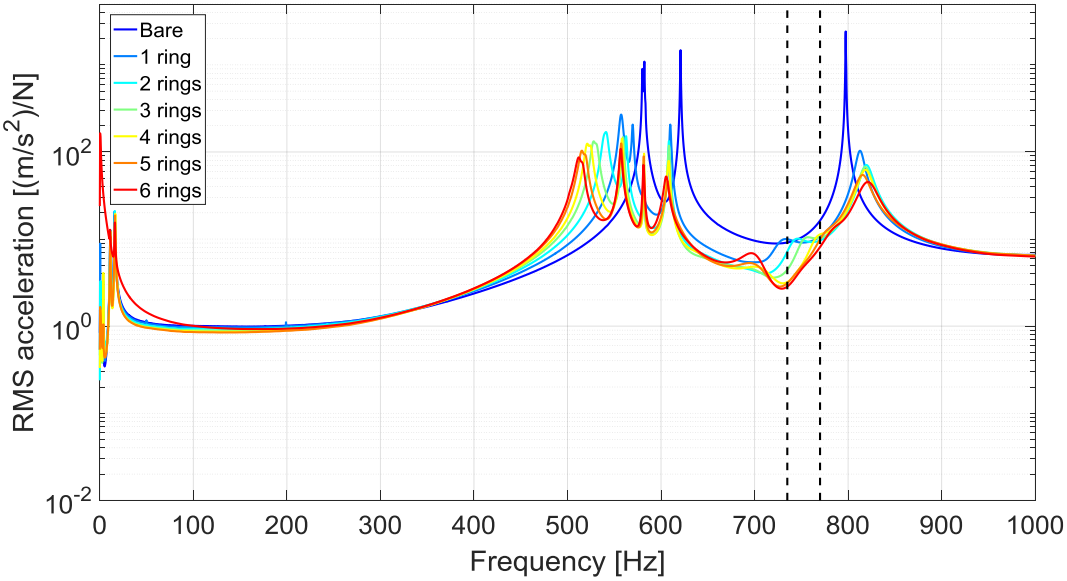

Figure 12: Frequency response of the RMS acceleration of all of the points through the length of the pipe with various numbers of resonator rings based on input on the location of accelerometer 1. Dashed lines indicate the numerically predicted stopband zone.

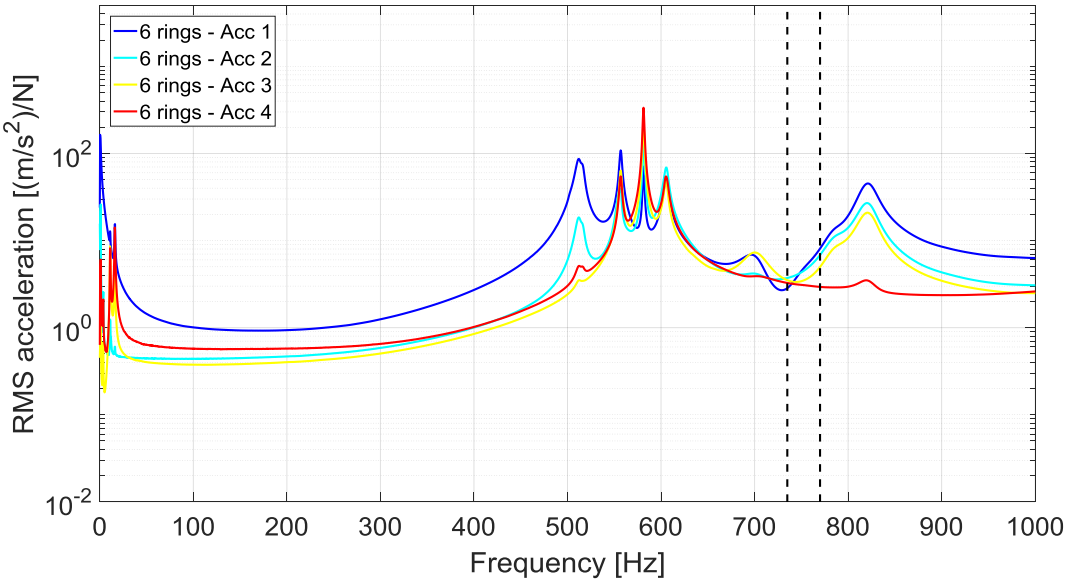

Figure 13: Frequency response of the RMS acceleration of all of the excitation point through the length of the bare pipe and the metamaterial pipe with 6 resonator rings based on input on the location of different accelerometers. Dashed lines indicate the numerically predicted stopband zone.

Fig. (13) shows the RMS frequency response of all of the points on the pipe with 6 rings based on input on the location of accelerometers 1 to 4. As it can be observed, the dip representing the stopband zone can be clearly detected in the measured response of the accelerometers 1 to 3. However, in the case of accelerometer 4 the dip is not as clear. As it can be seen, the amplitude of the response in the frequency range of the stopband is lower in the curve corresponding to accelerometer 4 compared to the other curves which can mask the dip related to

the stopband. Therefore, it is important to study the behavior of the section which contains this point, i.e. section 13, to verify the effect of the resonators on the opposite end of the pipe.

However in addition to the RMS response of the entire pipe, it is important to study the RMS response in different sections of the pipe. This section-wise investigation can provide a better understanding of the wave decay due to the addition of the resonator rings and can also assure a consistent reduction in the acceleration response of the pipe along its entire length. Fig. (14) provides the RMS response of the sections 1, 3, 5, 7, 10 and 13 for the metamaterial pipe with 6 added resonator rings. As it can be seen, the comparison of the responses of sections 1 – 7, that are in the region of the added resonant cells, clearly show that the dip in the stopband zone becomes more pronounced as the wave travels along the pipe and passes through each resonant cell. However, the observation of the dip due to the stopband in sections 10 and 13 (right at the opposite end of the pipe), in which resonant cells are not attached, proves that the metamaterial solution is influencing the frequency response of the entire pipe as expected.

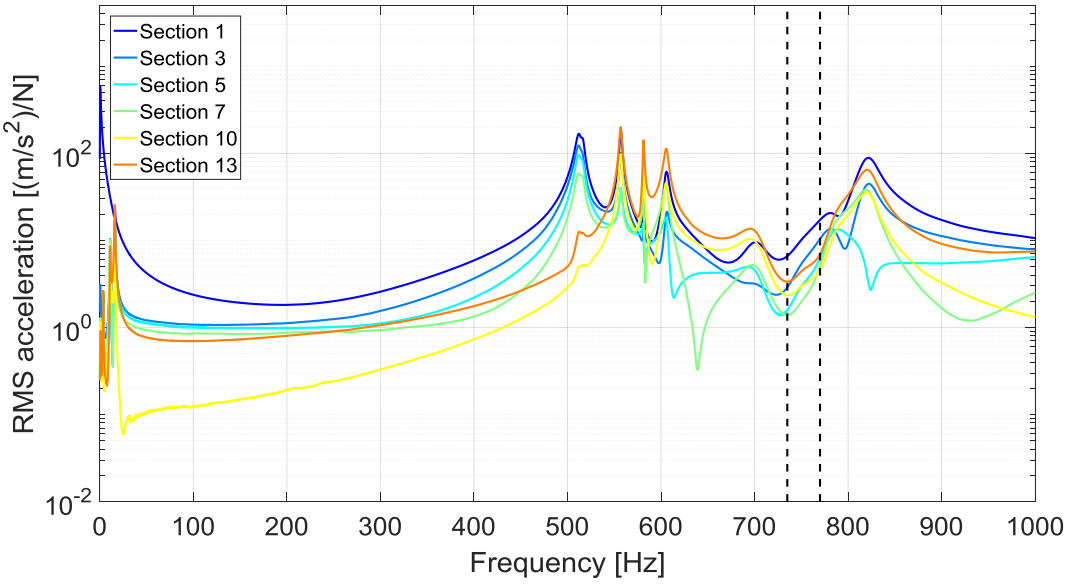

Figure 14: Frequency response of the RMS acceleration of various sections of the metamaterial pipe with 6 resonator rings based on input on the location of accelerometer 1. Dashed lines indicate the numerically predicted stopband zone.

Figs. (15) – (18) provide the frequency response of the pipe treated with different numbers of resonator rings in sections 1, 3, 7 and 13 based on input on the location of accelerometer 1, respectively. Results in these sections are presented as they provide a good understanding of the behavior of the metamaterial pipe as sections 1, 3 and 7 are located before, in between and behind the resonator rings and section 13 is the end of the pipe with no resonators attached. Considering that the pipe is treated with the metamaterial solution only at one end, it is important to study the effect of the resonators on its opposite end.

It is observed in Fig. (15) that in section 1 which is located before the resonator rings, the frequency responses due to a different number of resonator rings are not much influenced in the stopband zone. This can be explained due to the fact that both measurement and excitation points are before the resonator rings and therefore, this sections observes the effect of the rings minimally. The main difference between the pipe with different number of resonators comes from the additional mass of extra resonators which causes a frequency shift as ex-

plained before. However, in the response of the section 3 as shown in Fig. (16), there is a more considerable difference in the frequency response of the pipes with different number of resonator cells in the stopband zone. In this case, the pipes with more than two resonator rings show a more pronounced stopband zone. This observation becomes even more prominent for the response of the metamaterial with 6 resonator ring in section 7 as shown in Fig. (17). Considering that section 7 is located after the 6 resonator rings, the decay of the propagating waves becomes more pronounced with the addition of each resonator ring.

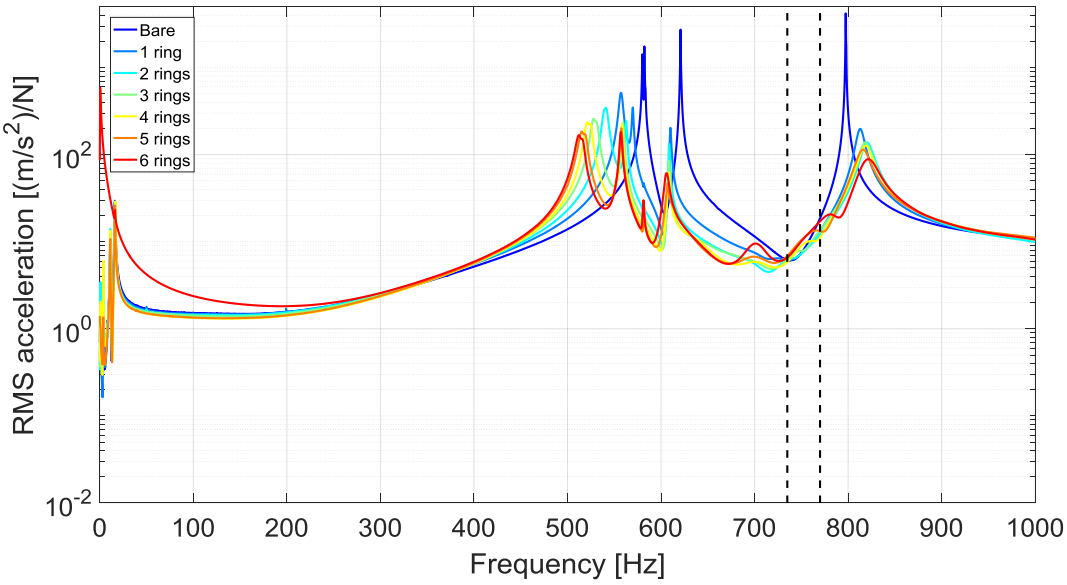

Figure 15: Frequency response of the RMS acceleration of section 1 of the pipe with various number of resonator rings corresponding to the excitation point located at accelerometer 1. Dashed lines indicate the numerically predicted stopband zone.

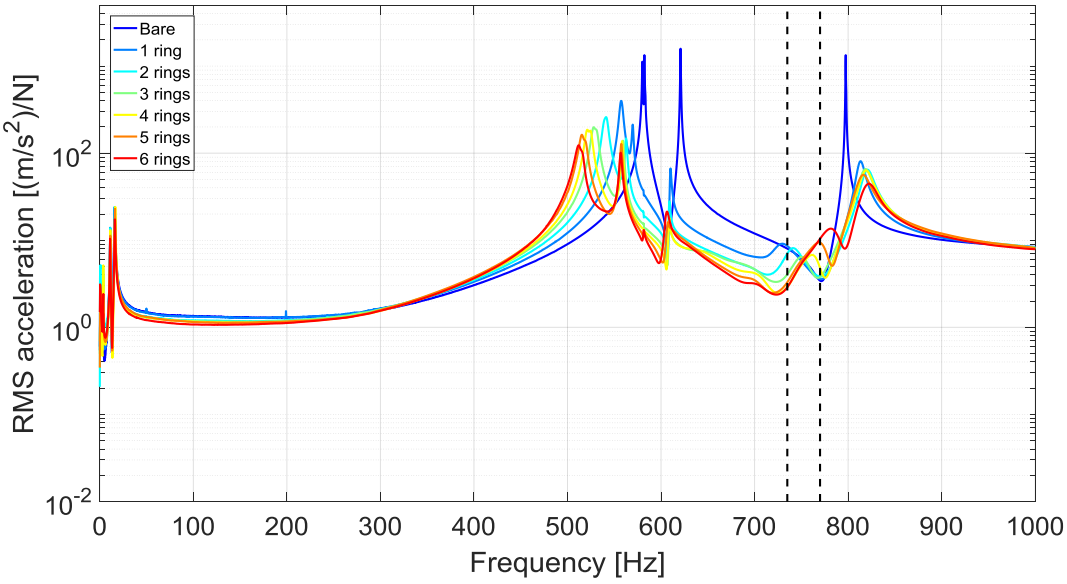

Figure 16: Frequency response of the RMS acceleration of section 3 of the pipe with various number of resonator rings corresponding to the excitation point located at accelerometer 1. Dashed lines indicate the numerically predicted stopband zone.

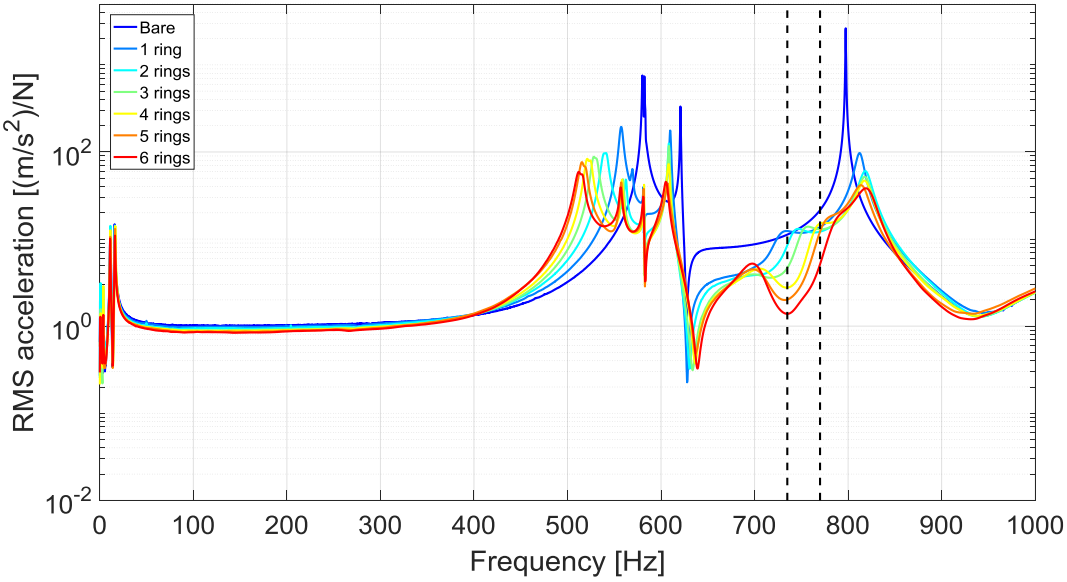

Figure 17: Frequency response of the RMS acceleration of section 7 of the pipe with various number of resonator rings corresponding to the excitation point located at accelerometer 1. Dashed lines indicate the numerically predicted stopband zone.

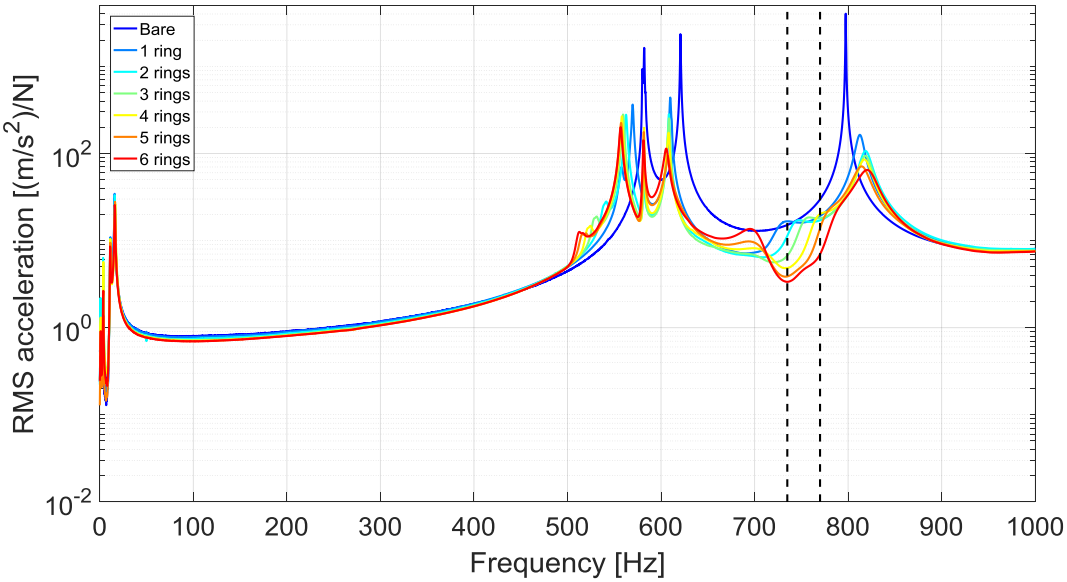

Figure 18: Frequency response of the RMS acceleration of section 13 of the pipe with various number of resonator rings corresponding to the excitation point located at accelerometer 1. Dashed lines indicate the numerically predicted stopband zone.

Frequency response functions obtained from section 13 as shown in Fig. (18), once more proves that the stopband zone is also obtained on the opposite end of the pipe in which again, the stopband dip becomes more pronounced with the addition of each resonator ring and the peaks representing different modes of the pipe become significantly damped after the addition of 6 resonator rings similar to section 7. In addition to the observations with respect to the stopband zone, as it can be seen in all of the figures, it is observed that the addition of the res-

onator rings causes a significant attenuation in the dynamic modes of the pipe. This effect can be more clearly observed at the peak around 800 Hz for all of the shown four sections.

7 CONCLUSIONS

In this paper, wave motion in locally resonant metamaterial pipes is investigated. Given the complex dynamics of curved structures and considering the wide range of application of lightweight Aluminum pipes such a pipe is chosen as the case study and a metamaterial solution is designed and proposed. The metamaterial solution has the potential to efficiently improve the NVH behavior of the pipe by the introduction of a stopband zone. Using the Bloch-Floquet theorem, the unit cell modelling method is utilized to numerically predict the frequency range of this stopband zone. The proposed metamaterial solution is then produced by cutting resonators out of a PMMA panel using laser cutting technique and by gluing them to the host Aluminum pipe. The host and metamaterial pipes are tested using the impact testing method under roving hammer excitation. The response is measured in different sections of the pipe for different numbers of resonant cells added to the pipe. The measurement results clearly verify the existence of a stopband zone due to the metamaterial treatment of the pipe. Comparison of the response of the pipes with different number of resonator cells shows that a pronounced reduction in the vibrational response can be obtained with a limited number of resonator cells corresponding to a 6.16% added mass to the Aluminum pipe; however, it is worth mentioning that addition of more resonator cells can result in higher amount of attenuation while adding to the mass. The validation case shows that the metamaterial solution can also influence parts of the pipe which are not treated with resonant cells, providing an efficient lightweight solution for vibration attenuation and possibly sound radiation reduction.

ACKNOWLEDGEMENTS

This research was partially supported by Flanders Make, the strategic research center for the manufacturing industry. The Research Fund KU Leuven is gratefully acknowledged for its support. The research of E. Deckers is funded by a personal grant from the Research Foundation – Flanders (F.W.O.).

REFERENCES

[1] L. Fritschi, L. Brown, R. Kim, D. Schwela, S. Kephalopous, Burden of disease from environmental noise: Quantification of healthy life years lost in Europe. *WHO Regional Office for Europe*, 2011.

[2] F. Lemoult, N. Kaina, M. Fink, G. Lerosey, Wave propagation control at the deep subwavelength scale in metamaterials. *Nature Physics*, **9**, 55-60, 2012.

[3] X. Zhou, X. Liu, G. Hu, Elastic metamaterials with local resonances: an overview. *Theoretical and Applied Mechanics Letters,* **2**, 2012.

[4] C. Goffaux, J. Sánchez-Dehesa, A. Yeyati, P. Lambin, A. Khelif, J. Vasseur, B. Djafari-Rouhani, Evidence of fano-like interference phenomena in locally resonant materials. *Physical Review Letters,* **88** (22), 2002.

[5] C. Claeys, P. Sas, W. Desmet, On the acoustic radiation efficiency of local resonance based stop band materials. *Journal of Sound and Vibration,* **333** (14), 3203-3213,

2014.

[6] C. Claeys, K. Vergote, P. Sas, W. Desmet, On the potential of tuned resonators to obtain low-frequency vibrational stop bands in periodic panels. *Journal of Sound and Vibration,* **332** (6), 1418–1436, 2013.

[7] T. Wang, M.P. Sheng, Z.W. Guo, Q.H. Qin, Flexural wave suppression by an acoustic metamaterial plate. *Applied Acoustics, Elsevier*, **114**, 118-124, 2016.

[8] C. Sugino, S. Leadenham, M. Ruzzene, A. Erturk, On the mechanism of bandgap formation in locally resonant finite elastic metamaterials. *Journal of Applied Physics*, **120**, 2016.

[9] C. Claeys, E. Deckers, B. Pluymers, W. Desmet, A lightweight vibro-acoustic metamaterial demonstrator: Numerical and experimental investigation. *Mechanical Systems and Signal Processing*, **70-71**, 853-880, 2016.

[10] C. Claeys, N. Rocha de Melo Filho, L. Van Belle, E. Deckers, W. Desmet, Design and validation of metamaterials for multiple structural stopbands in waveguides. *Extreme Mechanics Letters,* **12**, 7-22, 2017.

[11] F. Bloch, Über die Quantenmechanik der Electron in Kristallgittern. *Zeitschrift für Physik,* **52**, 550–600, 1928.

[12] G. Floquet, Sur les équations différentielles linéaires a coefficients périodiques. *Annales de l'Ecole Normale Supérieure*, **12**, 47–88, 1883.

[13] C. Collet, M. Ouisse, M. Ruzzene, M. Ichchou, Floquet–Bloch decomposition for the computation of dispersion of two-dimensional periodic, damped mechanical systems. *International Journal of Solids and Structures,* **48**, 2837–2848, 2011.

[14] A. Khelif, B. Aoubiza, S. Mohammadi, A. Adibi, V. Laude, Complete band gaps in two-dimensional phononic crystal slabs. *Physical Review E*, **74** (5), 2006.

[15] E. Manconi, B. Mace, Wave characterization of cylindrical and curved panels using a finite element method. *The Journal of Acoustical Society of America,* **125** (1), 154-163, 2009.

[16] A. Nateghi, L. Van Belle, C. Claeys, E. Deckers, B. Pluymers, W. Desmet, Wave propagation in locally resonant cylindrically curved metamaterial panels. *International Journal of Mechanical Sciences,* Article in press.

[17] A. Nateghi, L. Van Belle, C. Claeys, E. Deckers, B. Pluymers, W. Desmet, Stopband behavior in infinite metamaterial pipes. *proceedings of ISMA2016*, Leuven, Belgium, September 19-21, 2016.

[18] F. Fahy, *Sound and structural vibration*, London: Academic Press, 1987.

[19] N. Rocha de Melo Filho, C. Claeys, E. Deckers, B. Pluymers, W. Desmet, Dynamic Metamaterials for Structural Stopband Creation. *proceedings of International Styrian Noise, Vibration & Harshness Congress*, Graz, Austria, June 22-24, 2016.

[20] C. Claeys, *Design and analysis of resonant metamaterials for acoustic insulation*, Ph.D. dissertation, KU Leuven, Leuven, April 2014.